

Dual-polarization C-band Radar Measurements and Characterization of Hail in Finland between 2012 and 2015

Jani Tyynelä, Annakaisa von Lerber and Jari-Petteri Tuovinen



Introduction

During the summer months, hail is commonly observed in thunderstorms typically coming from south-west to Finland along the Atlantic air current. One of the objectives in the EU/Tekes funded Optimal Rain Products with Dual-Pol Doppler Weather Radar (OSAPOL) -project is to reduce the error due to hail when evaluating rainfall rate and accumulation from remote-sensing radar observations.

In this study, we have utilized citizen reports of hail in Finland between 2012 and 2015 and compared the observed hail size, place, and time of occurrence to corresponding radar measurements using the network of C-band dual-polarization radars operated by the Finnish Meteorological Institute (FMI). Figures in Panel 1 show some example photographs of the hail stones taken by the citizens.

For each radar volume, we measure reflectivity Z , differential reflectivity Z_{dr} , specific differential phase K_{dp} , and the amplitude of the copolarized correlation coefficient ρ_{hv} . In the figures on Panel 2, the relative frequency of each radar observable is shown. Notice that we also show the frequency for the different hydrometeor types classified by the HydroClass product.

The radar volumes are divided based on hail size into four categories (10 mm intervals) and based on the altitude of the volumes below/above the 0-degree-Celsius isotherm into four layers (1 km intervals) similar to the classification by [2013b]. Figures in Panel 3 show the contour levels of a combination of radar observables. The distributions are close to those at S-band [2013b], but with significantly larger values for the differential reflectivity. This is due to the resonances at 8 and 30 mm sizes [2013a].

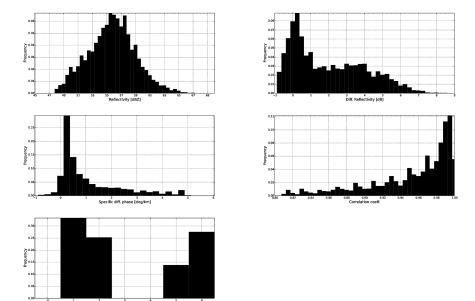
Finally, on Panel 4, we show two example cases of hail observations in Finland during the 19th of May, 2014. In the figures, we show the differences between Z-based and K_{dp} -based rainfall-rate estimations. The raingauge measurements for that day indicate that K_{dp} -based estimation is more accurate for the hail peaks than Z-based estimation. However, it is also clear that K_{dp} -based estimation fails before and after the hail peaks.

Panel 1. Hail images



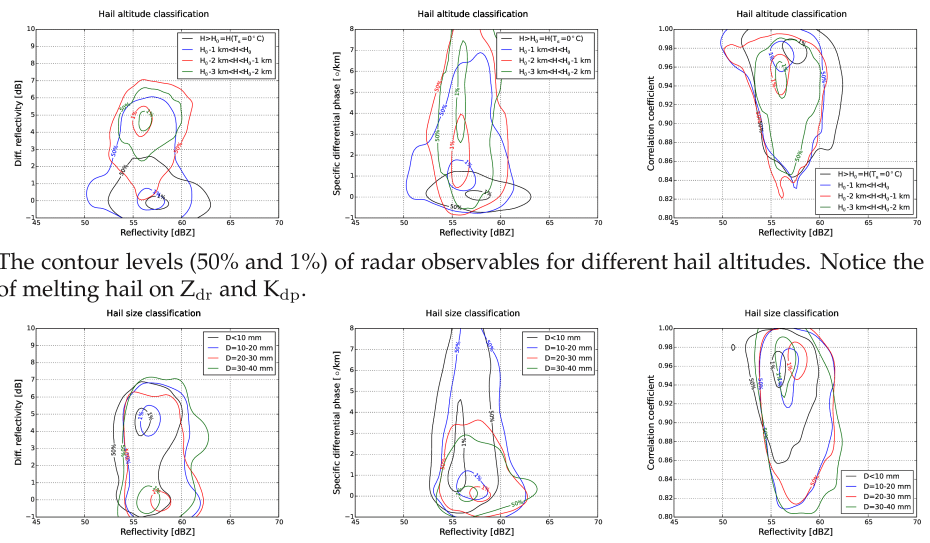
Example photographs of the hail stones reported by citizens.

Panel 2. Radar observables



Frequency plots for Z (top-left figure), Z_{dr} (top-right figure), K_{dp} (mid-left figure), ρ_{hv} (mid-right figure), and the HydroClass (No data: 0, Non-met: 1, Rain: 2, Wet-snow: 3, Snow: 4, Graupel: 5, Hail: 6) product (bottom figure).

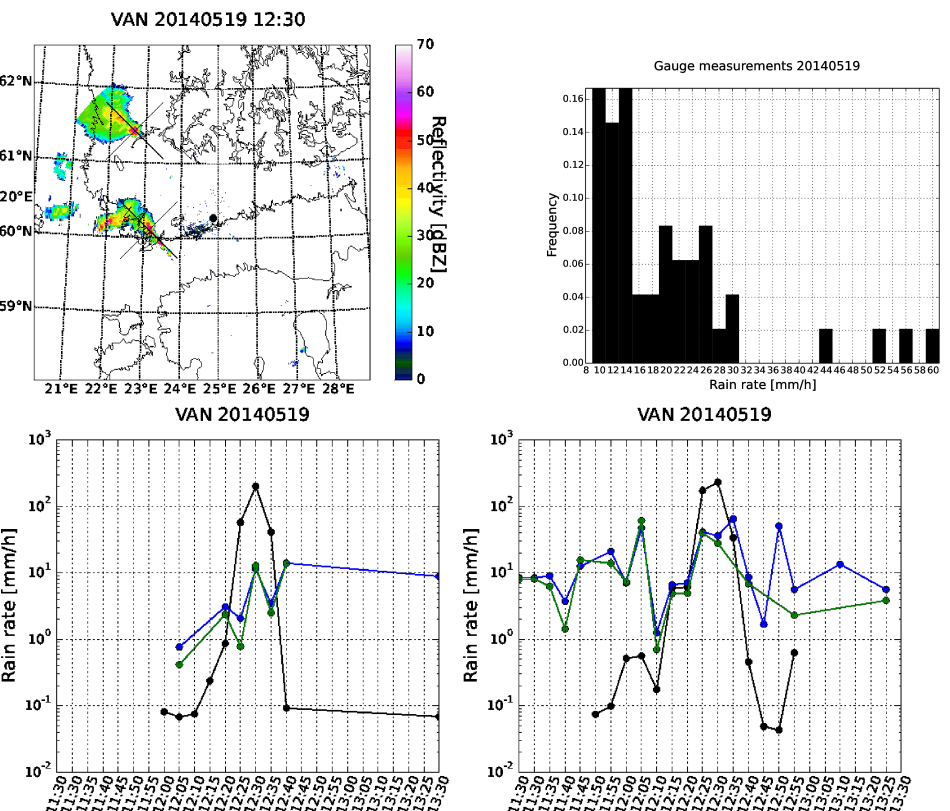
Panel 3. Radar observables divided by hail size and altitude



The contour levels (50% and 1%) of radar observables for different hail altitudes. Notice the effect of melting hail on Z_{dr} and K_{dp} .

The contour levels of radar observables for different hail sizes. Notice the sudden change in the 1% levels for Z_{dr} at $D = 20$ mm.

Panel 4. Hail time series for 19th May 2014



Two hail cells observed from the Vantaa radar (top-left figure). Raingauge measurements for the same day (top-right figure). Radar-based rainfall estimates using $R(Z)$ (black lines), $R(K_{dp})$ (blue lines) and $R(K_{dp}, Z_{dr})$ (green lines) relationships (bottom figures). Notice that the optimal thresholds between Z-based and K_{dp} -based relationships for the two cases may be different.

Acknowledgments

This work was funded by the EU/Tekes Optimal Rain Products with Dual-Pol Doppler Weather Radar (OSAPOL) -project.

References

2013a: Ryzhkov A. V., M. R. Kumjian, S. M. Ganson, and A. P. Khan (2013), Polarimetric Radar Characteristics of Melting Hail. Part I: Theoretical Simulations Using Spectral Microphysical Modeling, *J. Appl. Meteor. Clim.* **52**, 2849-2870
 2013b: Ryzhkov A. V., M. R. Kumjian, S. M. Ganson, and P. Zhang (2013), Polarimetric Radar Characteristics of Melting Hail. Part II: Practical Implications, *J. Appl. Meteor. Clim.* **52**, 2871-2886